

John J. Bates*

NOAA/NESDIS National Climatic Data Center, Asheville, North Carolina

1. INTRODUCTION

In order to separate the natural and anthropogenic effects of climate change, it is important to understand and quantify feedback mechanisms. Any process that changes the sensitivity of the climate response to an imposed anthropogenic forcing is called a feedback mechanism. Feedback mechanisms can either increase (a positive feedback) or decrease (a negative feedback) the magnitude of the climate response to forcing agents. For example, given the magnitude of a man-made greenhouse gas such as CO₂, the relationship between the magnitude of this anthropogenic climate forcing and the magnitude of the climate change response in a general circulation model, perhaps a global warming of 2°C, defines the climate sensitivity.

Large uncertainties occur in the feedback processes associated with clouds and water vapor, particularly in the Tropics. This is because in the Tropics there is a very large range in outgoing longwave radiation (OLR) between cold, high clouds near the Tropical tropopause and the clear, warm and dry atmospheres in the subtropical deserts. Recent papers have documented large variability in outgoing longwave radiation on both short and long time scales. Wielicki *et al.* (2002) find both large temporal (white in frequency space) variability in broadband OLR and a significant decadal trend. The white frequency variability is approximately $\pm 2 \text{ Wm}^{-2}$ for the tropical strip 20N-20S. The trends they find include a drop of about 2 Wm^{-2} from the late 1970s to the mid 1980s and a rise of about 4 Wm^{-2} from the late 1980s to the late 1990s. Work by Chen *et al.* (2002) examine possible mechanisms for the OLR trends documented by Wielicki and find this trend in OLR is consistent with changes in cloudiness and upper tropospheric humidity that suggest a decadal-time-scale strengthening of the tropical Hadley-Walker circulation. A closer examination of the Wielicki *et al.* (2002) time series of tropical OLR, however, also reveals high variability on subseasonal to seasonal time scales. Causes for this scale of variability were not fully examined by Wielicki *et al.* nor by Chen *et al.* (2002).

My examination of multiple satellite-derived indices and re-analysis over the past two decades suggests that there are important interactions between the different temporal scales due to the unique dynamical wave modes in the tropics. In the tropics, a dynamical wave duct opens in the northern winter and spring seasons such that mid-latitude Rossby waves can propagate deep into the subtropics and, sometimes, between hemispheres. The amount of this wave activity strongly affects the water and energy budget of the tropics and is a function of El Niño-Southern Oscillation (ENSO) state and mid-latitude transient activity. This discovery indicates that one must examine both changes in the transient tropical circulation modes, not just changes in the mean Hadley-Walker circulation, when seeking mechanisms to explain the large observed changes in the tropical water and energy cycle.

2. INTRASEASONAL TO INTERANNUAL VARIABILITY

Tropical (30°N-30°S) average time series of sea surface temperature, SST, [Reynolds, 1994], tropospheric temperature from the TOVS Microwave Sounding Unit (MSU channel 2) [Christy *et al.*, 1998; Christy *et al.*, 1995], upper tropospheric humidity (UTH), and Clear-sky OLR from ECMWF 15-year Re-Analysis (CLERA) [Sligo *et al.*, 1998] and Clouds and the Earth's Radiant Energy System (CERES) [Wielicki *et al.*, 1998] are shown in Figure 1. For this study of short frequency variability, the OLR data sets have been detrended and normalized. Also included in these plots are SST indices for the tropical Pacific regions sensitive to ENSO, the Niño 4 region in the western equatorial Pacific and the Niño 3 region in the central equatorial Pacific.

Although the correlations between SST and UTH and between SST and clear-sky OLR are not significant, there does appear to be some association between the different time series. The two most extreme negative values of UTH (most extreme positive value of clear-sky OLR) occur during the mature phase of the extreme ENSO events of 1982-83 and 1997-98. The most extreme positive value of UTH (most extreme negative value of clear-sky OLR) occurs during the extreme cold event of 1989. These UTH extremes are of much shorter duration than the SST and tropospheric temperature anomalies. This suggests that anomalies in tropical UTH and clear-sky OLR occur on both seasonal and interannual time scales in

*Corresponding author address: Dr. John Bates, National Climatic Data Center NOAA/NESDIS, 151 Patton Ave., Asheville, NC 28801; email: John.J.Bates@noaa.gov

contrast to SST and tropospheric temperature which show only interannual variability.

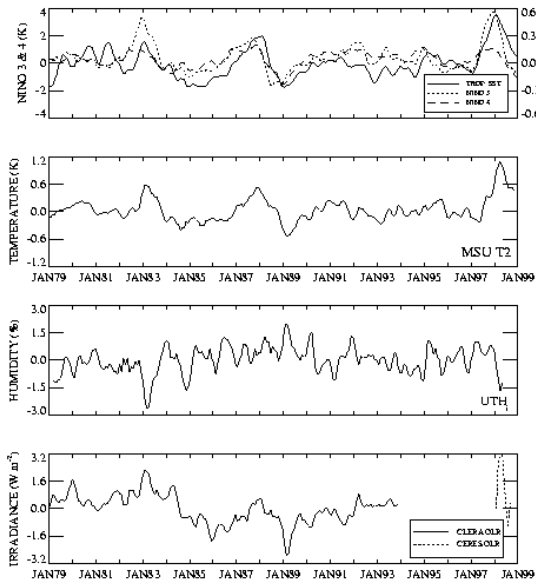


Figure 1. Tropical (30N-30S) indices of a) sea surface temperature, b) lower tropospheric temperature (MSU2R), c) upper tropospheric humidity, and d) outgoing longwave radiation (OLR).

In an attempt to identify which regions of the tropics contribute most significantly to the tropical wide time series of figure 1c, a one-point correlation map between the tropical-wide UTH time series and the UTH time series was computed at each grid point.

This map (Figure 2; note due to truncation of the graphics, the magnitude of the 1998 ENSO is truncated) shows that the largest contribution comes from the eastern Pacific (Bates et al. 2001; Bates et al., 1996). Several studies have indicated that transient eddy activity is high in this area [Kiladis and Weickmann, 1997] and that the transient eddies are associated with large plumes of moisture [Iskenderian, 1995]. This transient eddy activity has a strong seasonal component [Kiladis and Weickmann, 1997] and also shows a strong interaction with ENSO events [Matthews and Kiladis, 1999]. Thus, variations in eddy activity are a possible candidate to explain some extremes of the tropical interannual anomaly time series of UTH and clear-sky OLR.

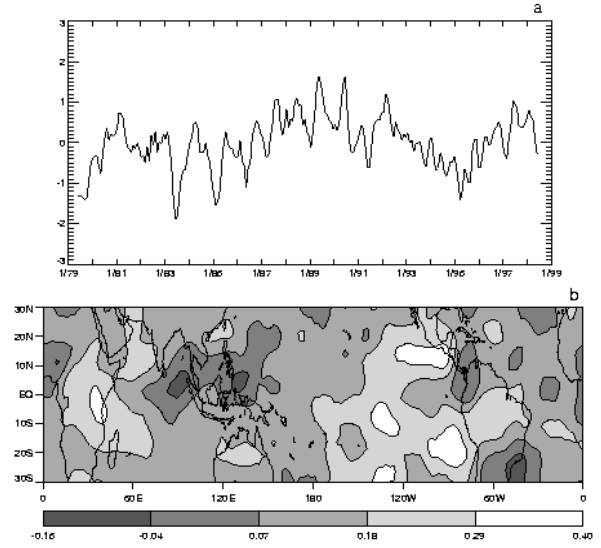


Figure 2. Interannual anomaly of UTH (a) and one-point correlation map (b).

3. PROPAGATION OF MID-LATITUDE ROSSBY WAVES INTO THE TROPICS AND THE ROLE OF THE WESTERLY DUCT

To examine the changes in transient eddy activity in this region during the large warm event of 1982-83 and the large cold event of 1989-90, we employed the dynamical analysis of 200 hPa winds as outlined in Kiladis [1998]. The horizontal E vector is a pseudo-vector constructed by calculating time-mean covariances between the perturbation zonal, u' , and meridional, v' , wind components:

$$\vec{E} = \left(\overline{v'^2 - u'^2}, -\overline{u'v'} \right) \quad (1)$$

The term $\overline{v'^2 - u'^2}$ is a measure of the mean anisotropy of Rossby waves. For example, if v'^2 is consistently larger than u'^2 , the Rossby waves are preferentially elongated in the meridional direction and the E-vector points eastward. The term $-\overline{u'v'}$ is the negative of the time-mean northward flux of westerly momentum associated with perturbations. Together the two components approximate the preferred direction of the group velocity of the Rossby waves using suitable approximations, including the assumption of quasi-geostrophy. For this work, we use the NCEP re-analysis data and bandpass filter for 6-30 day transients.

Another useful diagnostic for representing the mean background state in which the transients are embedded is the stationary Rossby wavenumber:

$$K_s = \left(\frac{\beta_*}{\bar{U}} \right)^{1/2} \quad (2)$$

$$\text{where } \beta_* = \beta - \frac{\partial^2 \bar{U}}{\partial y^2} \quad (3)$$

is the meridional gradient of absolute vorticity associated with the basic flow, \bar{U} is the monthly mean 200 hPa zonal wind, and $\beta = \frac{\partial f}{\partial y}$ is the meridional gradient of planetary vorticity. K_s is the total wavenumber at which a barotropic Rossby wave is stationary at a particular location in a given background zonal flow. Low values of the stationary Rossby wave number (below about 10) indicate regions of strong eddy activity and high values (above 15) indicate regions of weak eddy activity.

E-vectors and the stationary Rossby wavenumber were computed for all months and plots of the minima UTH (April 1983) and maxima UTH (February 1989) months are shown in Figure 3.

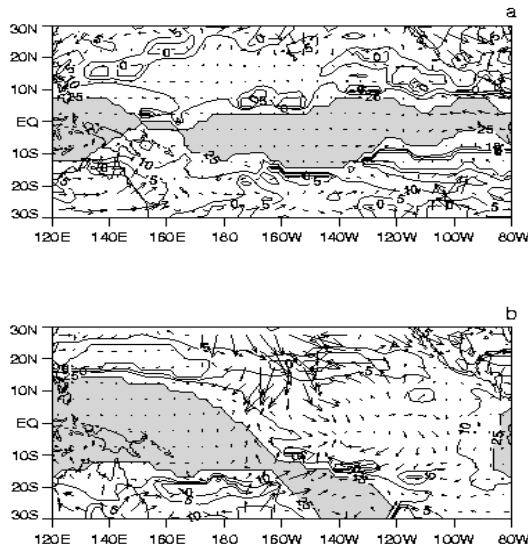


Figure 3. E-vectors and stationary Rossby wave numbers for February of 1983 (a) and January of 1989 (b).

In the northern hemisphere, mid-latitude interactions with the tropics are greatest in boreal winter and spring when transient Rossby wave activity with periods between 5 and 30 days is at a peak. During strong cold events, such as 1989 (Figure 3b), tropical convection occurs only over the far western Pacific Ocean since the western Pacific warm pool shrinks and moves to the west during cold events. In the tropical upper troposphere near the equator, this creates strong westerly winds in

the outflow from this convection over the central and eastern Pacific. This allows the opening of a westerly duct in the eastern Pacific and supports propagation of Rossby waves deep into the subtropics [Webster and Holton, 1982]. This is evidenced in Figure 3b where values of stationary Rossby wave numbers less than 10 are found in the regions between the dateline and the west coast of South America. Large values of E-vectors pointing toward the equator near Hawaii are indicative of equatorially-propagating Rossby waves from the mid-latitudes into the subtropics. As shown by Kiladis [1998], the Rossby waves then propagate to the east and are associated with large plumes of moisture extending from near Hawaii to the U.S. west coast sometimes dubbed the 'pineapple express'.

Conversely, during the large warm event of 1982 (Figure 3a), deep convection extends far to the east in the equatorial Pacific Ocean. Upper tropospheric westerlies over the equator weaken dramatically or even reverse in the central and eastern Pacific. This is confirmed by calculations of the stationary Rossby wave number for these events. Large values of the stationary Rossby wave number are found over the eastern tropical Pacific, effectively shutting down the westerly duct. Virtually no E-vectors pointing toward the equator are found in this month, indicating an almost complete absence of Rossby waves in the subtropical North Pacific.

The statistical characteristics of the relationship between the UTH extremes and Rossby wave activity were examined by computing the seasonal mean Rossby stationary wave number. I computed the mean of all months within the season for only those months within the season with tropical average UTH anomalies greater than 0.7% and UTH anomalies less than -0.7%. For the boreal spring season (Figure 4), low values of the stationary Rossby wave number extend further west versus the mean along the equator when UTH anomalies exceed 0.7% (Figure 4b) and are found further east when UTH anomalies are less than -0.7% (Figure 4c). The situation is similar for the boreal winter season. Thus, the westerly duct is larger when UTH anomalies exceed 0.7% and is much smaller when UTH anomalies are less than -0.7%.

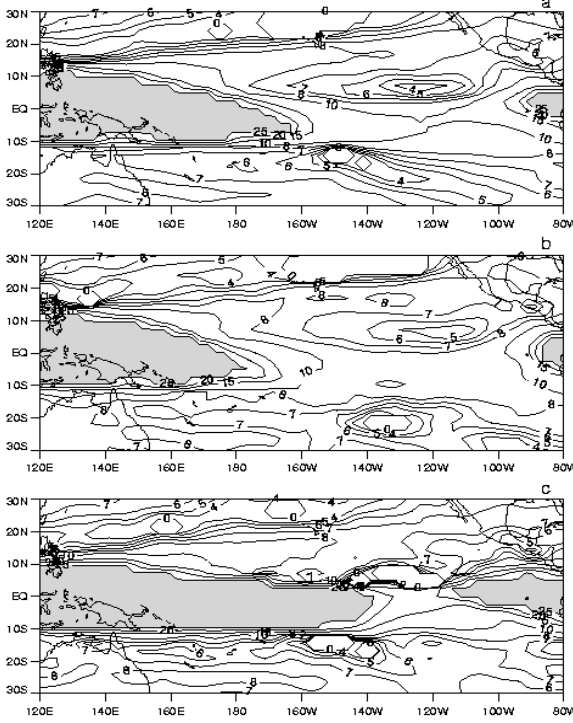


Figure 4. Stationary Rossby wave number corresponding to normal UTH (a), high extremes of UTH (b), and low extremes of UTH (c).

4. EFFECTS ON THE TROPICAL WATER BUDGET

The budget equation for water vapor is

$$\frac{Dq}{Dt} = s(q) + D \quad (4)$$

Where $s(q)$ is the rate of generation or destruction of water vapor and D is the molecular and eddy diffusion through the boundaries. Expanding (4) in sigma coordinates we get

$$\frac{Dq}{Dt} = \left(\frac{\partial q}{\partial t} + \vec{v} \cdot \nabla q \right)_{\sigma} + \sigma \frac{\partial q}{\partial \sigma} \quad (5)$$

Where the total derivative of specific humidity has been decomposed into the local time rate of change in specific humidity, horizontal and vertical advection terms. Introducing mass continuity and writing in flux form, the water vapor balance equation can be written

$$\frac{Dq}{Dt} = \frac{\partial q}{\partial t} + \nabla \cdot (\vec{v}q) + \frac{\partial(\dot{\sigma}q)}{\partial \sigma} + q \left[\frac{\partial \ln p_s}{\partial t} + \vec{v} \cdot \nabla \ln p_s \right] \quad (6)$$

The local time tendency, horizontal and vertical flux components of (6) are analogous to the water vapor equation in pressure coordinates; however, an additional surface pressure tendency term and a horizontal advection of surface pressure term account for variations in surface pressure. These terms are negligible over the ocean.

Water vapor mass flux was computed for an arbitrary sized box defined by longitude coordinates λ_1 and λ_2 , latitude coordinates ϕ_1 and ϕ_2 , and vertical coordinates σ_1 and σ_2 . The zonal water vapor mass flux through a meridional plane was defined

$$\int_{\phi_1}^{\phi_2} \frac{p_s(\lambda, \phi)}{g} \left(\int_{\sigma_1}^{\sigma_2} (uq)_{\lambda} d\sigma \right) r d\phi \quad (7)$$

Where P_s is surface pressure, g is acceleration due to gravity, and r is the earth's radius. Likewise for the meridional water vapor flux through a zonal plane

$$\int_{\lambda_1}^{\lambda_2} \frac{P_s(\phi, \lambda)}{g} \left(\int_{\sigma_1}^{\sigma_2} (\overline{vq})_{\phi} d\sigma \right) r \cos \phi d\lambda \quad (8)$$

And the vertical flux through a surface defined on sigma level (sigma)

$$\int_{\phi_1}^{\phi_2} \left(\int_{\lambda_1}^{\lambda_2} \frac{\sigma p_s(\lambda, \phi)}{g} (\dot{\sigma}q)_{\sigma} d\lambda \right) r^2 \cos \phi d\phi \quad (9)$$

This study focuses on the horizontal region defined by 160E-150W, 15N-25N and the vertical region defined between the sigma levels of 0.5 and 0.2; a region with climatological high OLR indicating significant energy loss to space. It is generally accepted that the vertical flow in this region is dominated by subsidence, which will dry the upper troposphere and allow significant amount of energy to escape to space. To balance this drying process, water vapor needs to be transported either horizontally or vertically into this region. To investigate this balance, we to computed the monthly water vapor mass flux for each side of the box over the a 17-yr period (a longer time series will be available soon) using the computed monthly mean total moisture flux data. Summation of the

six terms results in a net divergence/convergence of water vapor in the region.

A detailed examination of the monthly moisture flux in this region indicates 39% of the months over the 17-yr period have a mean downward vertical motion field but a mean upward vertical moisture flux in the upper troposphere. Figure 5 gives time series of the region-mean vertical velocity and the total, stationary and transient vertical moisture flux for the 0.5-0.2 sigma layer. Whereas the climatology of the vertical velocity is downward, the vertical moisture flux is upward with all the mean flux contribution coming from the transient vertical flux. Therefore, transient disturbances of less than 30 days contribute almost entirely to the climatological mean upward water vapor flux found in this subtropical region. In fact, 79% of the months with downward motion and upward moisture flux also have downward stationary moisture flux. Therefore, it is entirely the transient moisture flux which contributes to upward moisture flux in these cases. This transient upward flux is strong enough to contribute significantly to the total vertical moisture flux such that upward flux occurs. Further verification of this result was performed by computing each term of water vapor balance equation at each grid point in the box. Integration of the water vapor tendency, horizontal and vertical divergence terms achieved the same result as the flux calculation.

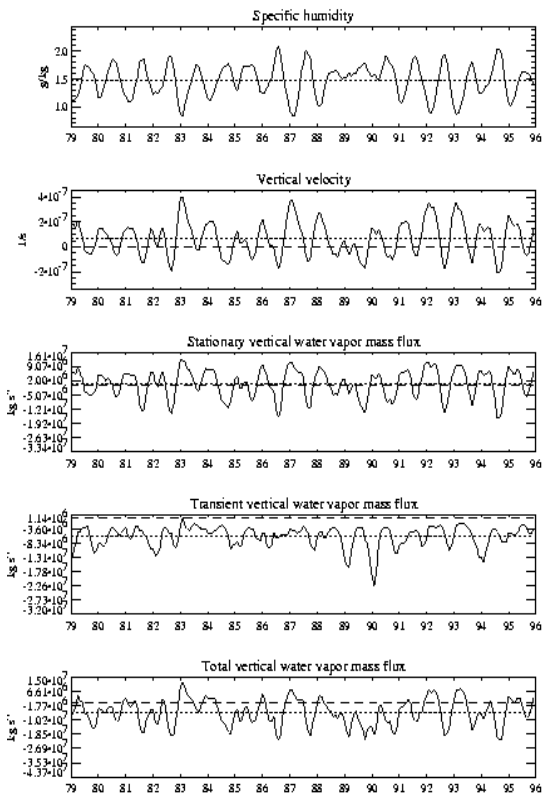


Figure 5. Components of the vertical water vapor mass flux for the subtropical North Pacific.

5. CONCLUSIONS

Atmospheric dynamical states, resulting from the interaction of the tropics with the mid-latitudes during boreal winter and spring, are responsible for most of the observed extremes in the tropical UTH time series. These states are referred to as the westerly duct in the eastern Pacific Ocean. The two extreme states of the westerly duct, and their influence on UTH, are illustrated schematically in figure 6.

During extremes of high UTH (Figure 6a), strong westerlies flowing out from deep convection in the western equatorial Pacific create a long fetch of westerlies over the equatorial eastern Pacific. This opens the westerly duct and allows Rossby waves (strong eddy activity) to propagate into the subtropics and re-hydrate the subtropical upper troposphere. Conversely, when deep convection extends into the central and eastern Pacific (Figure 6b), westerly winds over the tropical eastern Pacific are weak and Rossby waves are blocked from propagating into the subtropics (no eddies).

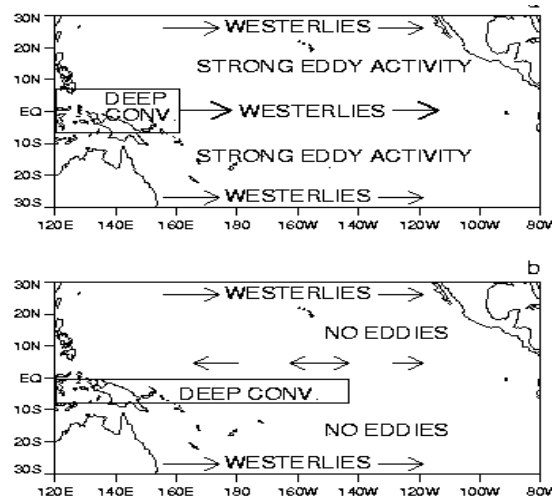


Figure 6. Schematic of tropical basic states for extremes of high UTH (a) and low UTH (b).

Hypotheses for mechanisms that control the water and energy budget of the tropics often refer only to the effects of the Hadley and Walker cells in causing the observed variability. This is equivalent to ignoring the effects of transient eddies. Analysis of the water and energy budgets, however, demonstrates that transient eddies contribute significantly to the water and energy budgets and, thus, can not be ignored. Instead, the contribution of transient eddies must be included, but these

contributions may be understood within the lower frequency regimes of seasonal to interannual variability.

5. REFERENCES

- Bates, J.J., D.L. Jackson, F.-M. Breon, and Z.D. Bergen, Variability of upper tropospheric humidity 1979-1998, *Journal of Geophysical Research*, 106 (D23), 23,271-23,282, 2001.
- Bates, J.J., X. Wu, and D.L. Jackson, Interannual variability of upper-tropospheric water vapor band brightness temperature, *Journal of Climate*, 9 (2), 427-438, 1996.
- Chen, J., B. E. Carlson, and A. D. Del Genio, Evidence for strengthening of the Tropical general circulation in the 1990s. *Science*, 295, 838-841, 2002.
- Christy, J.R., R.W. Spencer, and E.S. Lobl, Analysis of the merging procedure for the MSU daily temperature time series, *Journal of Climate*, 11, 2016-2041, 1998.
- Christy, J.R., R.W. Spencer, and R.T. McNider, Reducing Noise in the MSU Daily Lower-Tropospheric Global Temperature Dataset, *Journal of climate*, 8 (4), 888-902, 1995.
- Iskenderian, H., A 10-year climatology of Northern Hemisphere tropical cloud plumes and their composite flow patterns, *Journal of Climate*, 8, 1630-1637, 1995.
- Kiladis, G.N., Observations of Rossby Waves Linked to Convection over the Eastern Tropical Pacific, *Journal of the atmospheric sciences*, 55 (3), 321, 1998.
- Kiladis, G.N., and K.M. Weickmann, Horizontal Structure and Seasonality of Large-Scale Circulations Associated with Submonthly Tropical Convection, *Monthly weather review*, 125 (9), 1997-2008, 1997.
- Matthews, A.J., and G.N. Kiladis, Interactions between ENSO, Transient Circulation, and Tropical Convection over the Pacific, *Journal of climate*, 12 (10), 3062-3074, 1999.
- Reynolds, R.W.S., T. M., Improved sea surface temperature analysis using optimum interpolation, *Journal of Climate*, 7, 929-937, 1994.
- Slingo, A., J.A. Pamment, and M.J. Webb, A 15-year simulation of the clear-sky greenhouse effect using the ECMWF reanalyses: fluxes and comparisons with ERBE, *Journal of Climate*, 11 (4), 690-706, 1998.
- Webster, P.J., and J.R. Holton, Cross-equatorial response to middle-latitude forcing in a zonally varying basic state, *Journal of the Atmospheric Sciences*, 39 (4), 722-733, 1982.
- Wielicki, B.A., B.R. Barkstrom, B.A. Baum, T.P. Charlock, R.N. Green, D.P. Kratz, R.B. Lee Iii, P. Minnis, G.L. Smith, T. Wong, D.F. Young, R.D. Cess, J.A. Coakley Jr, D.A.H. Crommelynck, L. Donner, R. Kandel, M.D. King, A.J. Miller, V. Ramanathan, D.A. Randall, L.L. Stowe, and R.M. Welch, Clouds and the Earth's Radiant Energy System (CERES): Algorithm Overview, *IEEE transactions on geoscience and remote sensing*, 36 (4), 1127-1136, 1998.
- Wielicki, B. A. and co-authors, Evidence for large decadal variability in the Tropical mean radiative energy budget, *Science*, 295, 841-844.